Int. J. Heat Mass Transfer. Vol. 31, No. 4, pp. 769–777, 1988
Printed in Great Britain

0017–9310/88 $3.00+0.00

The flow and vortex instability of horizontal natural convection in a porous medium resulting from combined heat and mass buoyancy effects

JIIN-YUH JANG and WEN-JENG CHANG
Department of Mechanical Engineering, National Cheng-Kung University, Tainan, Taiwan 70101, Republic of China

(*Received* 16 *March* 1987 *and in final form* 31 *August* 1987)

Abstract—An analysis is performed to study the flow and the vortex instability of natural convection in a porous medium that results from simultaneous diffusion of heat and mass in a boundary layer adjacent to a horizontal surface. Numerical results for the Nusselt number, Sherwood number, and the neutral stability curves are presented for Lewis numbers ranging from 1 to 10 and the buoyancy ratio in the range of -0.5 to 4. For mass transfer aiding the flow, the results indicate that the Nusselt number and Sherwood number are higher than those for pure thermal convection and the flow is more susceptible to the vortex instability, while for mass transfer opposing the flow, the opposite trend is true. The critical thermal Rayleigh number is found to increase with decreasing Lewis number.

1. INTRODUCTION

THERE ARE many natural convections in porous media which occur in natural and in technological applications in which flows are driven simultaneously by the differences in temperature and concentration. The applications include the migration of moisture through the air contained in the fibrous insulations and the grain storage installations, and the dispersion of chemical contaminants through water-saturated soil.

Bejan and Khair [1] analysed the vertical natural convection boundary layer flow in a porous medium resulting from the combined buoyancy mechanism. The natural convection phenomenon occurring inside a porous enclosure with both heat and mass transfer from the side was studied by Trevisan and Bejan [2]. Raptis *et al.* [3] studied the influence of free convection flow and mass transfer on the steady flow of a viscous fluid through a porous medium, which is bounded by a vertical infinite plate, when the temperature and concentration on the plate are kept constant.

The onset of convection of the flow in a horizontal porous layer with imposed vertical temperature and concentration gradient has been the subject of studies by Nield [4], Gershuni *et al.* [5] and Turner and Gustafson [6]. The wave mode and vortex mode of instability of a horizontal and inclined natural convection boundary layer of a viscous fluid under the combined buoyancy effects were examined by Pera and Gebhart [7] and Chen *et al.* [8], respectively. Hsu *et al.* [9] and Hsu and Cheng [10] analysed the vortex mode of instability of horizontal and inclined natural convection flows in a porous medium caused solely by a single buoyancy effect, namely, the effect of temperature variation. However, the vortex mode of instability of a natural convection in a porous medium along a horizontal surface, under the combined thermal and mass diffusion processes, seems not to have been investigated. This motivates the present investigation. As might be expected, the results for a porous medium resemble those for a viscous fluid. However, there are some differences, notably those arising from the boundary conditions and the governing equations that differ in the two problems.

2. MATHEMATICAL ANALYSIS

2.1. *The base flow*

Before proceeding to the instability problem, consideration is given first to the basic natural convection flow along a horizontal surface, since the computation of instability criteria requires a knowledge of the velocity, temperature and concentration profiles for the main flow and the solution has not been investigated before.

The base flow analysis treats a semi-infinite, horizontal isothermal (T_0) and isoconcentration (C_0) surface embedded in a saturated porous medium at temperature T_∞ ($<T_0$) and concentration C_∞ ($<C_0$). The physical situation is shown in Fig. 1, where x represents the distance along the plate from the leading edge and y represents the distance normal to the surface.

The following conventional assumptions simplify the analysis.

(1) The physical properties are considered to be constant, except for the density term that is associated with the body force.

(2) Flow is sufficiently slow that the convecting

NOMENCLATURE

a	dimensional spanwise wave number
C	mass fraction of the diffusing species
C'	perturbation mass fraction of the diffusing species
$\tilde{C}$	disturbance mass fraction amplitude
D	mass diffusivity
f	similarity stream function profile
g	gravitational acceleration
k	dimensionless wave number
K	Darcy permeability
L	length of wall
Le	Lewis number, α/D
N	buoyancy ratio
Nu	Nusselt number, $q'/k_1(T_0-T_\infty)$
Nu_x	local Nusselt number
P, P'	main flow, perturbation pressure
Ra_L	Rayleigh number, $Kg\beta L(T_0-T_\infty)/\alpha\nu$
Ra_x	local Rayleigh number
Sh	Sherwood number, $j'/D(C_0-C_\infty)$
Sh_x	local Sherwood number
t	time
T	temperature
T'	perturbation temperature
$\tilde{T}$	disturbance temperature amplitude
$\tilde{u}$	x-direction disturbance velocity amplitude
u, v, w	Darcy's velocity in x-, y-, z-direction
u', v', w'	axial, normal, and spanwise components of velocity disturbances
x, y, z	axial, normal, and spanwise coordinates.

Greek symbols

α	effective thermal diffusivity
β_c, β_T	coefficients of concentration, thermal expansion
δ_c, δ_T	concentration, thermal boundary layer thickness
η	similarity variable
θ	dimensionless temperature
Θ	dimensionless disturbance temperature amplitude
λ	dimensionless mass fraction
Λ	dimensionless disturbance mass fraction amplitude
μ, ν	absolute, kinematic viscosity
ξ	volumetric heat capacity of the saturated porous medium to that of the fluid
ρ	density
σ	temporal growth constant
ϕ	porosity of the medium
ψ	stream function
ψ'	disturbance stream function
$\tilde{\psi}$	disturbance stream function amplitude
Ψ	dimensionless disturbance stream function amplitude.

Superscripts

*	critical condition
¯	main flow quantity
~	amplitude function for disturbance.

Subscripts

0	condition at the wall
∞	condition at the free stream.

fluid and the porous matrix are in local thermodynamic equilibrium.

(3) The processes occur at low concentration difference such that the diffusion-thermo and thermodiffusion effects and the interfacial velocity due to mass diffusion can be neglected.

(4) Darcy's law, the Boussinesq and boundary layer approximations are employed.

The equations that account for the conservation of mass, momentum, energy and concentration according to the above assumptions are

$$\frac{\partial u}{\partial x}+\frac{\partial v}{\partial y}=0 \tag{1}$$

$$\frac{\partial u}{\partial y}=-\frac{\rho_\infty Kg}{\mu}\left(\beta_T\frac{\partial T}{\partial x}+\beta_c\frac{\partial C}{\partial x}\right) \tag{2}$$

$$u\frac{\partial T}{\partial x}+v\frac{\partial T}{\partial y}=\alpha\frac{\partial^2 T}{\partial y^2} \tag{3}$$

$$u\frac{\partial C}{\partial x}+v\frac{\partial C}{\partial y}=D\frac{\partial^2 C}{\partial y^2} \tag{4}$$

where K is the permeability of the saturated porous medium; β_T and β_c are the coefficients for thermal and concentration expansion; α and D represent the equivalent thermal and mass diffusivity. Other various symbols are defined in the Nomenclature.

The boundary conditions for the above set of equations are simple if we neglect any induced velocity at the surface caused by the mass diffusion effect. They are

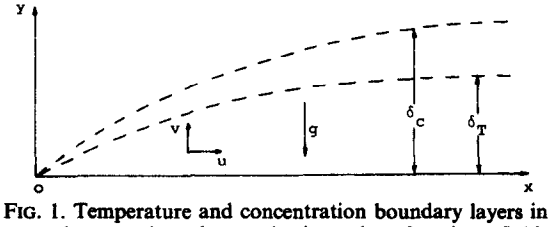

FIG. 1. Temperature and concentration boundary layers in natural convection along a horizontal surface in a fluid-saturated porous medium.

$$\text{at } x = 0, \quad u = 0, \quad T = T_\infty, \quad C = C_\infty$$
$$\text{at } y = 0, \quad v = 0, \quad T = T_0, \quad C = C_0$$
$$\text{as } y \to \infty, \quad u \to 0, \quad T \to T_\infty, \quad C \to C_\infty. \tag{5}$$

On introducing the following transformation:

$$\eta = \frac{y}{x} Ra_x^{1/3}, \quad \psi = \alpha\, Ra_x^{1/3} f(\eta)$$
$$\theta = \frac{T - T_\infty}{T_0 - T_\infty}, \quad \lambda = \frac{C - C_\infty}{C_0 - C_\infty} \tag{6}$$

where $Ra_x = g\beta_T K x (T_0 - T_\infty)/\alpha\nu$ is the modified local thermal Rayleigh number, and ψ is the stream function which automatically satisfies equation (1), the following similarity equations are obtained:

$$f'' - \frac{2}{3}\eta(\theta' + N\lambda') = 0 \tag{7}$$

$$\theta'' + \frac{1}{3} f\theta' = 0 \tag{8}$$

$$\lambda'' + \frac{Le}{3} f\lambda' = 0. \tag{9}$$

In the above equations, the primes indicate the derivative with respect to the similarity variable η; $Le = \alpha/D$ is the Lewis number; N the buoyancy ratio which is defined as

$$N = \frac{\beta_c (C_0 - C_\infty)}{\beta_T (T_0 - T_\infty)}. \tag{10}$$

When $N = 0$, equations (7) and (8) reduce to those equations for flow over a horizontal flat plate without mass transfer [11].

Following the scale analysis as described by Bejan and Khair [1], the flow, heat/mass transfer and boundary layer thickness scales can be obtained as shown in Table 1. It is seen that the streamwise velocity (u) scales for the heat-transfer-driven and mass-transfer-driven flows are $u_T \sim \alpha\, Ra_L^{2/3}/L$ and $u_m \sim \alpha(Ra_L|N|)^{2/3} Le^{-1/3}/L$, respectively. Therefore, the flow becomes dominated by heat buoyancy when $N^2/Le < 1$ (i.e. $u_T > u_m$) and by mass buoyancy when $N^2/Le > 1$ (i.e. $u_T < u_m$). When $N < 0$ and $N^2/Le \simeq 1$, the flow violates the boundary layer assumptions because in this range the temperature and concentration buoyancy effects are of the same order of magnitude and in opposite directions.

The boundary conditions are transformed as follows:

$$f(0) = 0, \quad \theta(0) = 1, \quad \lambda(0) = 1$$
$$f'(\infty) = 0, \quad \theta(\infty) = 0, \quad \lambda(\infty) = 0. \tag{11}$$

In terms of the dimensionless variables, it can be easily shown that the local Nusselt number and Sherwood number are given by

$$Nu_x = -\theta'(0)\, Ra_x^{1/3} \tag{12}$$
$$Sh_x = -\lambda'(0)\, Ra_x^{1/3}. \tag{13}$$

2.2. *The disturbance flow*

The standard method of linear stability theory in which the instantaneous values of velocity, pressure, temperature and concentration components are perturbed by small amplitude disturbances and the mean flow quantities subtracted, with terms higher than first order in disturbance quantities being neglected, results in the following equations:

$$\frac{\partial u'}{\partial x} + \frac{\partial v'}{\partial y} + \frac{\partial w'}{\partial z} = 0 \tag{14}$$

$$u' = -\frac{K}{\mu}\frac{\partial P'}{\partial x} \tag{15}$$

$$v' = -\frac{K}{\mu}\left[\frac{\partial P'}{\partial y} - \rho(\beta_T T' + \beta_c C')g\right] \tag{16}$$

$$w' = -\frac{K}{\mu}\frac{\partial P'}{\partial z} \tag{17}$$

$$\xi\frac{\partial T'}{\partial t} + \bar{u}\frac{\partial T'}{\partial x} + u'\frac{\partial \bar{T}}{\partial x} + \bar{v}\frac{\partial T'}{\partial y} + v'\frac{\partial \bar{T}}{\partial y} = \alpha\left(\frac{\partial^2 T'}{\partial x^2} + \frac{\partial^2 T'}{\partial y^2} + \frac{\partial^2 T'}{\partial z^2}\right) \tag{18}$$

$$\phi\frac{\partial C'}{\partial t} + \bar{u}\frac{\partial C'}{\partial x} + u'\frac{\partial \bar{C}}{\partial x} + \bar{v}\frac{\partial C'}{\partial y} + v'\frac{\partial \bar{C}}{\partial y} = D\left(\frac{\partial^2 C'}{\partial x^2} + \frac{\partial^2 C'}{\partial y^2} + \frac{\partial^2 C'}{\partial z^2}\right) \tag{19}$$

where the barred and primed quantities signify the mean flow and disturbance flow components, respectively, ξ is the volumetric heat capacity of the saturated porous medium to that of the fluid, and ϕ the porosity of the medium.

Following the method of order-of-magnitude analysis prescribed in detail by Hsu and Cheng [10] for free convection flow over an inclined surface in a porous medium without mass transfer, the terms

Table 1. Flow, heat/mass transfer and boundary layer thickness scales near a horizontal wall in a porous medium with combined buoyancy effects

Driving mechanism	u	δ_T	δ_c	Nu	Sh	Observations
Heat transfer	$\alpha\, Ra_L^{2/3}/L$	$L\, Ra_L^{-1/3}$	$L\, Le^{-1/2} Ra_L^{-1/3}$	$Ra_L^{1/3}$	$Ra_L^{1/3} Le^{1/2}$	$Le \gg 1$
$\lvert N\rvert \ll 1$	$\alpha\, Ra_L^{2/3}/L$	$L\, Ra_L^{-1/3}$	$L\, Ra_L^{-1/3} Le^{-1}$	$Ra_L^{1/3}$	$Ra^{1/3} Le$	$Le \ll 1$
Mass transfer	$\alpha(Ra_L\lvert N\rvert)^{2/3} Le^{-1/3}/L$	$L(Ra_L\lvert N\rvert)^{-1/3} Le^{1/6}$	$L(Ra_L Le\lvert N\rvert)^{-1/3}$	$(Ra_L\lvert N\rvert)^{1/3} Le^{-1/6}$	$(Ra_L Le\lvert N\rvert)^{1/3}$	$Le \ll 1$
$\lvert N\rvert \gg 1$	$\alpha(Ra_L\lvert N\rvert)^{2/3} Le^{-1/3}/L$	$L(Ra_L\lvert N\rvert)^{-1/3} Le^{2/3}$	$L(Ra_L Le\lvert N\rvert)^{-1/3}$	$(Ra_L\lvert N\rvert)^{1/3} Le^{-2/3}$	$(Ra_L Le\lvert N\rvert)^{1/3}$	$Le \gg 1$

$\partial u'/\partial x$, $\partial^2 T'/\partial x^2$, $\partial^2 C'/\partial x^2$ in equations (14), (18) and (19) can be neglected. The omission of $\partial u'/\partial x$ in equation (14) implies the existence of a disturbance stream function ψ' such that

$$w' = \frac{\partial \psi'}{\partial y}, \quad v' = -\frac{\partial \psi'}{\partial z}. \tag{20}$$

We assume that the three-dimensional disturbances are of the form

$$(\psi', u', T', C') = [\tilde{\psi}(x,y), \tilde{u}(x,y), \tilde{T}(x,y), \tilde{C}(x,y)] \times \exp(iaz + \sigma t + \gamma(x)) \tag{21}$$

where a is the spanwise periodic wave number, σ the temporal growth factor while

$$\gamma(x) = \int \alpha_i(x)\,dx$$

with $\alpha_i(x)$ denoting the spatial growth factor. Substituting equation (21) into equations (15)–(19) and setting $\sigma = \alpha_i = 0$ for neutral stability yields

$$ia\tilde{u} = \frac{\partial^2 \tilde{\psi}}{\partial x \partial y} \tag{22}$$

$$\frac{\partial^2 \tilde{\psi}}{\partial y^2} - a^2\tilde{\psi} = -\frac{i\rho_\infty g K \beta_T a}{\mu}\left(\tilde{T} + \frac{\beta_c}{\beta_T}\tilde{C}\right) \tag{23}$$

$$\alpha\left(\frac{\partial^2 \tilde{T}}{\partial y^2} - a^2\tilde{T}\right) = \tilde{u}\frac{\partial \bar{T}}{\partial x} + \tilde{v}\frac{\partial \bar{T}}{\partial y} + \bar{u}\frac{\partial \tilde{T}}{\partial x} - ia\tilde{\psi}\frac{\partial \bar{T}}{\partial y} \tag{24}$$

$$D\left(\frac{\partial^2 \tilde{C}}{\partial y^2} - a^2\tilde{C}\right) = \tilde{u}\frac{\partial \bar{C}}{\partial x} + \tilde{v}\frac{\partial \bar{C}}{\partial y} + \bar{u}\frac{\partial \tilde{C}}{\partial x} - ia\tilde{\psi}\frac{\partial \bar{C}}{\partial y}. \tag{25}$$

Equations (22)–(25) are solved based on the local similarity approximations [10], wherein the disturbances are assumed to have weak dependence in the streamwise direction (i.e. $\partial/\partial x \ll \partial/\partial\eta$). We let

$$\begin{aligned} k &= ax/Ra_x^{1/3} \\ \Psi(\eta) &= \tilde{\psi}/i\alpha\, Ra_x^{1/3} \\ \Theta(\eta) &= \tilde{T}/(T_0 - T_\infty) \\ \Lambda(\eta) &= \tilde{C}/(C_0 - C_\infty). \end{aligned} \tag{26}$$

which gives the following system of equations for the local similarity approximations:

$$\Psi'' - k^2\Psi = -k\,Ra_x^{1/3}(\Theta + N\Lambda) \tag{27}$$

$$\Theta'' + \tfrac{1}{3}f\Theta' - k^2\Theta = \tfrac{2}{3}\eta\theta'[(2\eta\Psi'' + \Psi')/(k\,Ra_x^{1/3})] + k\,Ra_x^{1/3}\theta'\Psi \tag{28}$$

$$\Lambda'' + \tfrac{1}{3}Lef\Lambda' - k^2\Lambda = Le\{\tfrac{2}{3}\eta\lambda'[(2\eta\Psi'' + \Psi')/(k\,Ra_x^{1/3})] + k\,Ra_x^{1/3}\lambda'\Psi\} \tag{29}$$

with boundary conditions

$$\begin{aligned} \Theta(0) = \Lambda(0) = \Psi(0) = 0 \\ \Theta(\infty) = \Lambda(\infty) = \Psi(\infty) = 0 \end{aligned} \tag{30}$$

where the primes indicate the derivative with respect to η. Equations (27)–(30) constitute a sixth-order system of linear ordinary differential equations for the disturbance amplitude distributions $\Psi(\eta)$, $\Theta(\eta)$ and $\Lambda(\eta)$. For fixed Le and N, solutions Ψ, Θ and Λ are eigenfunctions for eigenvalues Ra_x and k.

3. NUMERICAL METHOD OF SOLUTION

In the stability calculations, the disturbance equations are solved by separately integrating three linearly independent integrals. The full equations may be written as the sum of three linearly independent solutions

$$\begin{aligned} \Psi &= \Psi_1 + B_2\Psi_2 + B_3\Psi_3 \\ \Theta &= \Theta_1 + B_2\Theta_2 + B_3\Theta_3 \\ \Lambda &= \Lambda_1 + B_2\Lambda_2 + B_3\Lambda_3. \end{aligned} \tag{31}$$

The three independent integrals $(\Psi_i, \Theta_i, \Lambda_i)$, with $i = 1, 2, 3$, may be chosen so that their asymptotic solutions are

$$\begin{aligned} \Psi_1 &= -\left(\frac{k}{A^2 - k^2}\right)Ra_x^{1/3}\exp(A\eta_\infty), \\ \Theta_1 &= \exp(A\eta_\infty), \quad \Lambda_1 = 0 \\ \Psi_2 &= -\left(\frac{Nk}{S^2 - k^2}\right)Ra_x^{1/3}\exp(s\eta_\infty), \\ \Theta_2 &= 0, \quad \Lambda_2 = \exp(s\eta_\infty) \\ \Psi_3 &= \exp(-k\eta_\infty), \quad \Theta_3 = 0, \quad \Lambda_3 = 0 \end{aligned} \tag{32}$$

where

$$\begin{aligned} A &= -\frac{1}{6}f_\infty - \left[\left(\frac{1}{6}f_\infty\right)^2 + k^2\right]^{1/2} \\ S &= -\frac{Le}{6}f_\infty - \left[\left(\frac{Le}{6}f_\infty\right)^2 + k^2\right]^{1/2}. \end{aligned} \tag{33}$$

A sixth-order Runge–Kutta, variable step size integration routine is used here to solve first the sixth-order base flow system, equations (7)–(9), and the results are stored for a fixed step size, $\Delta\eta = 0.02$, which is small enough to predict accurate linear interpolation between mesh points. Equations (27)–(29) with boundary conditions, equations (30), are then solved as follows. For specified Le, N and k, Ra_x is guessed. Using equations (32) as starting values, the three integrals are integrated separately from the outer edge of the boundary layer to the wall using a sixth-order Runge–Kutta variable size integrating routine incorporated with the Kaplan filtering technique [12] to maintain the linear independence of the eigenfunctions. The required input of the base flow to the disturbance equations is calculated, as necessary, by linear interpolation of the stored base flow. From the values of the integrals at the wall, B_2 and B_3 are determined using the boundary conditions $\Theta(0) = 0$ and $\Lambda(0) = 0$. The third boundary condition $\Psi(0) = 0$ is satisfied only for an appropriate value of the eigen-

value Ra_x. A Taylor series expansion of the third condition provides a correction scheme for the initial guess of Ra_x. Iterations continue until the third boundary condition is sufficiently close to zero ($<10^{-5}$, typically).

4. RESULTS AND DISCUSSIONS

Numerical results for base flow are obtained for $Le = 1$–100, with the buoyancy ratio N ranging from -4 to 4. The numerical values of $f'(0)$, $\theta'(0)$ and $\lambda'(0)$ for selected values of Le and N are tabulated in Table 2. For $N = 0$, the only contribution to the body force is due to thermal diffusion and the results are in good agreement with those of Cheng and Chang [11].

Figures 2–4 show the effects of the buoyancy ratio N on the velocity, temperature and concentration distributions for $Le = 1$ and 5. It is seen that the aiding ($N > 0$) and opposing ($N < 0$) buoyancy effects alter the form of these distributions. In Fig. 2, we observe that, for a given Le, the velocity is increased with increasing values of N. For a given aiding buoyancy ratio N (>0), the velocity is decreased as Le is increased, while for a given opposing buoyancy ratio N (<0), the velocity is increased as Le is increased.

Figures 3 and 4 illustrate that, for a fixed Le, an increase of the value of N results in a thinning of the temperature and concentration boundary layers. It is also shown that, for $N > 0$, the effect of increasing Le is to thicken the temperature boundary layer and to thin the corresponding concentration boundary layer, while for $N < 0$, the effect of increasing Le results in a thinning of both layers.

Figures 5 and 6 give the local Nusselt number and Sherwood number for $Le = 1$–100 for a range of N in both the aiding and opposing regions. It is observed from Fig. 5 that all the curves coincide at $N = 0$, i.e. for pure thermal convection. A positive N increases the heat transfer and the increment depends strongly on Le. For $N > 0$, as Le increases, the heat transfer is seen to decrease. This is because a larger Le provides a thicker thermal boundary layer as seen in Fig. 3. A negative N produces the opposite effect. Figure 6

Table 2. Summary of similarity solutions for slip velocity, local Nusselt and Sherwood numbers

Le	N	$f'(0)$	$-\theta'(0)$	$-\lambda'(0)$
1	−0.5	0.660	0.341	0.341
	0.0	1.054	0.430	0.430
	1.0	1.676	0.542	0.542
	2.0	2.196	0.621	0.621
	4.0	3.087	0.736	0.736
5	−1.5	0.395	0.337	0.716
	−1.0	0.665	0.379	0.862
	−0.5	0.874	0.408	0.960
	0.0	1.054	0.430	1.037
	1.0	1.369	0.465	1.160
	2.0	1.646	0.494	1.259
	4.0	2.134	0.539	1.416
10	−2.0	0.398	0.358	1.032
	−1.5	0.611	0.385	1.197
	−1.0	0.778	0.403	1.311
	−0.5	0.923	0.418	1.403
	0.0	1.054	0.43	1.481
	1.0	1.290	0.450	1.612
	2.0	1.501	0.467	1.722
	4.0	1.878	0.495	1.902
100	−4.0	0.650	0.415	3.908
	−2.0	0.870	0.424	4.372
	−1.0	0.965	0.427	4.558
	−0.5	1.011	0.429	4.644
	0.0	1.054	0.430	4.725
	1.0	1.138	0.433	4.878
	2.0	1.218	0.435	5.018
	4.0	1.368	0.440	5.272

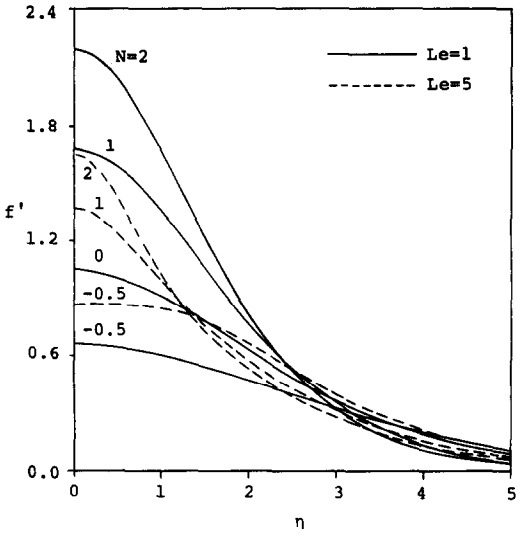

FIG. 2. Dimensionless velocity distribution vs η for selected values of N for $Le = 1$ and 5.

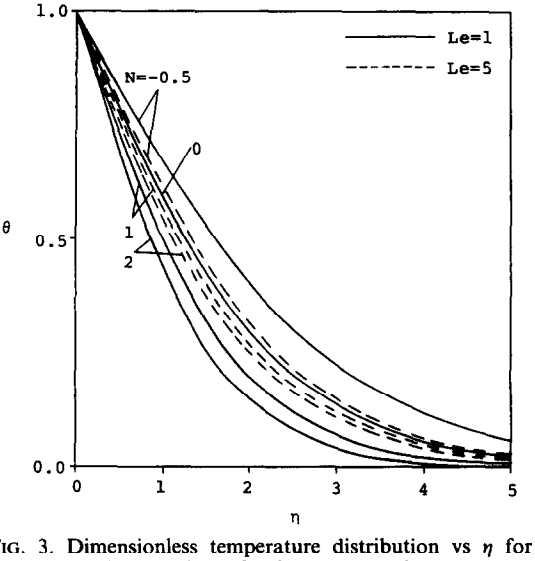

FIG. 3. Dimensionless temperature distribution vs η for selected values of N for $Le = 1$ and 5.

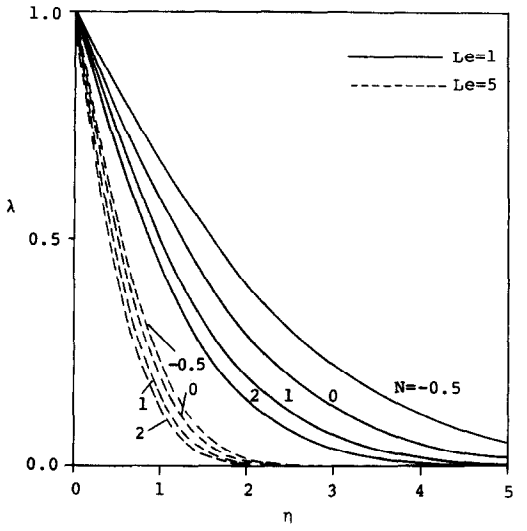

FIG. 4. Dimensionless concentration distribution vs η for selected values of N for $Le = 1$ and 5.

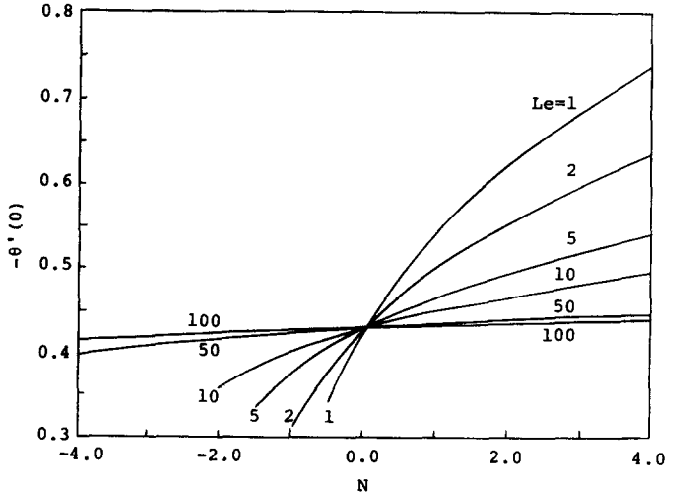

FIG. 5. Local Nusselt number as a function of N for different values of Le.

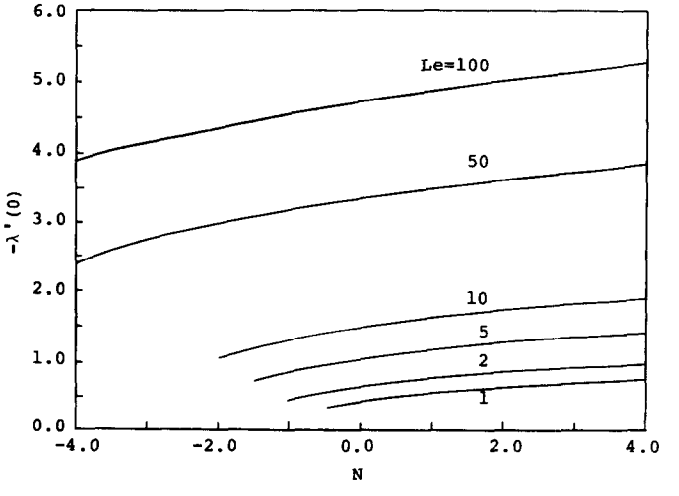

FIG. 6. Local Sherwood number as a function of N for different values of Le.

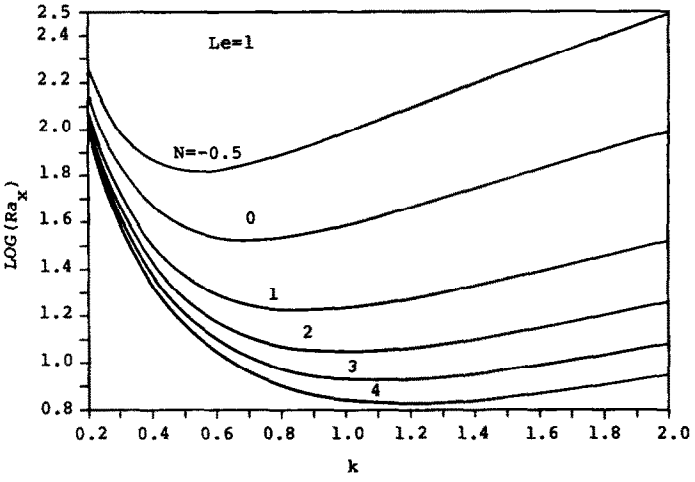

FIG. 7(a). Neutral stability curves for selected values of N, $Le = 1$.

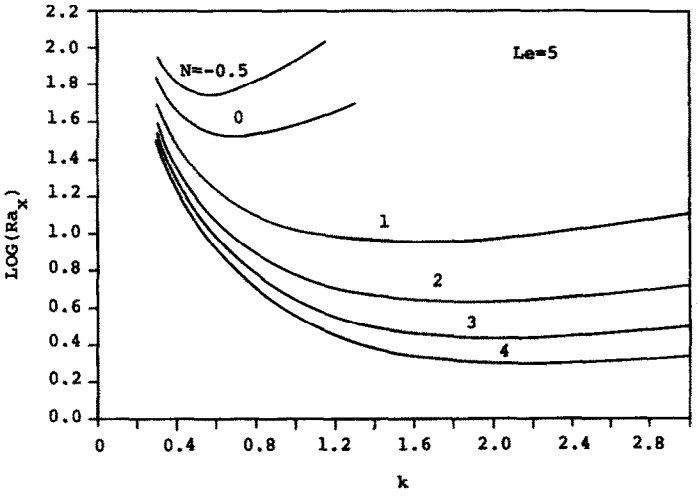

FIG. 7(b). Neutral stability curves for selected values of N, $Le = 5$.

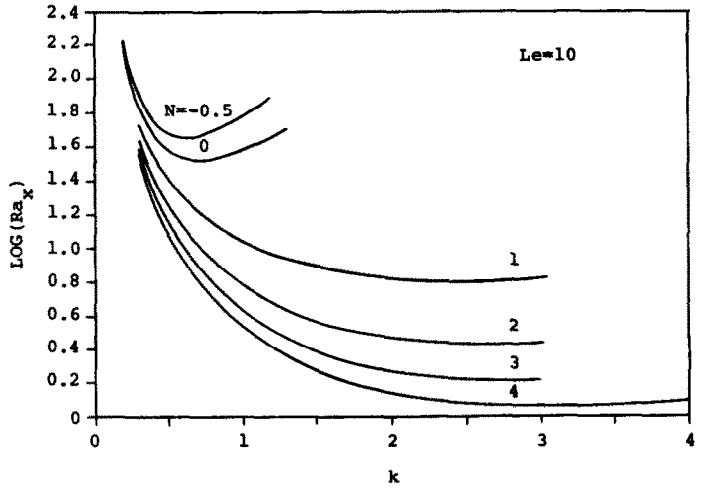

FIG. 7(c). Neutral stability curves for selected values of N, $Le = 10$.

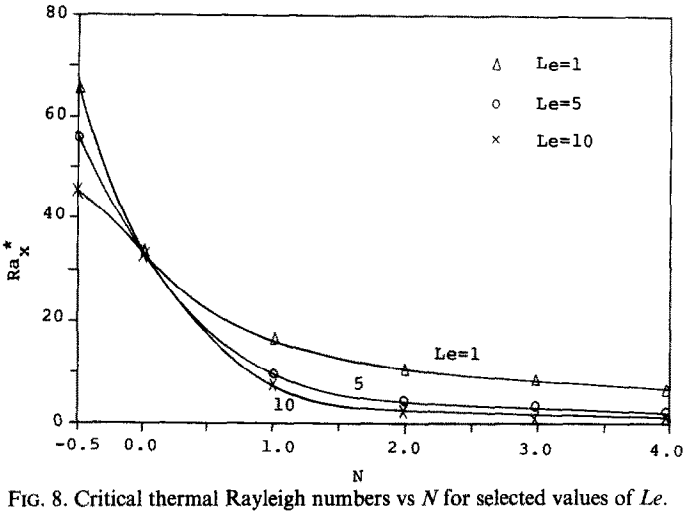

FIG. 8. Critical thermal Rayleigh numbers vs N for selected values of Le.

indicates that, when N is fixed, the surface mass transfer consistently increases as Le increases. This is because the concentration boundary layer becomes increasingly thinner as Le increases.

Figures 7(a)–(c) show the effect of the buoyancy ratio N on the neutral stability curves for $Le = 1$, 5 and 10, respectively. The instability of the flow is seen to be affected by the buoyancy force from mass diffusion. The neutral curves of Fig. 7 indicate that the greater the buoyancy ratio N, the more susceptible is the flow to the vortex mode of instability. In other words, under the combined buoyancy models, the disturbances are amplified more rapidly for increasing N. The variations of the critical thermal Rayleigh number Ra_x^* with the buoyancy ratio N for the three Lewis numbers, $Le = 1$, 5 and 10, are illustrated in Fig. 8. It is found that, whether the mass transfer is aiding or opposing the flow, the critical thermal Rayleigh number is consistently increased as the Lewis number is decreased.

5. CONCLUSIONS

This paper concerns the flow and vortex instability of a horizontal natural convection flow in a porous medium which arises due to the interaction of the force of gravity and density differences caused by the simultaneous diffusion of thermal energy and of chemical species. The base flow is assumed to be the steady, two-dimensional boundary layer flow, and the similarity solution is shown to exist. A linear perturbation analysis is employed in the formulation of the neutral stability equations. The numerical results indicate as the buoyancy force ratio increases, both the surface heat and mass transfer rates increase, causing the flow to become more susceptible to the vortex instability. The critical thermal Rayleigh number is found to be increased as the Lewis number is decreased.

REFERENCES

1. A. Bejan and K. R. Khair, Heat and mass transfer by natural convection in a porous medium, *Int. J. Heat Mass Transfer* **29**, 909–918 (1985).
2. O. V. Trevisan and A. Bejan, Natural convection with combined heat and mass transfer buoyancy effects in a porous medium, *Int. J. Heat Mass Transfer* **28**, 1597–1611 (1985).
3. A. Raptis, G. Tzivanidis and N. Kafousias, Free convection and mass transfer flow through a porous medium bounded by an infinite vertical limiting surface with constant suction, *Lett. Heat Mass Transfer* **8**, 417–424 (1981).
4. D. A. Nield, Onset of thermohaline convection in a porous medium, *Water Resour. Res.* **4**, 553–560 (1968).
5. G. Z. Gershuni, E. M. Zhukhovitshii and D. V. Lyubimov, Thermal concentration instability of a mixture in a porous medium, *Sov. Phys. Dokl.* **21**, 375–377 (1976).
6. J. S. Turner and L. B. Gustafson, The flow of hot saline solutions from vents in the sea floor—some implications for exhalative massive sulfide and other ore deposits, *Econ. Geol.* **73**, 1082–1100 (1978).
7. L. Pera and B. Gebhart, On the stability of natural convection boundary layer flow over horizontal and slightly inclined surface, *Int. J. Heat Mass Transfer* **16**, 1147–1163 (1973).
8. T. S. Chen, K. L. Tzuoo and A. Moutsoglou, Vortex instability of horizontal and inclined natural convection flows from simultaneous thermal and mass diffusion, *J. Heat Transfer* **105**, 774–781 (1983).
9. C. T. Hsu, P. Cheng and G. M. Homsy, Instability of free convection flow over a horizontal impermeable surface in a porous medium, *Int. J. Heat Mass Transfer* **21**, 1221–1228 (1978).
10. C. T. Hsu and P. Cheng, Vortex instability in buoyancy-induced flow over inclined heated surfaces in a porous media, *J. Heat Transfer* **101**, 660–665 (1979).
11. P. Cheng and I-Dee Chang, Buoyancy induced flows in a saturated porous medium adjacent to impermeable horizontal surfaces, *Int. J. Heat Mass Transfer* **19**, 1267–1272 (1976).
12. R. E. Kaplan, The stability of laminar incompressible boundary layers in the presence of complaint boundaries, M.I.T. Aeroelastic and Structures Research Laboratory, ASRL-TR 116-1 (1964).

INSTABILITE D'ECOULEMENT ET DE TOURBILLON POUR UNE CONVECTION NATURELLE HORIZONTALE DANS UN MILIEU POREUX ET RESULTANT D'EFFETS FLOTTANTS COMBINES DE CHALEUR ET DE MASSE

Résumé—Une étude est conduite sur l'écoulement et l'instabilité de vortex en convection naturelle dans un milieu poreux, résultant de la diffusion simultanée de chaleur et de masse dans une couche limite adjacente à une surface horizontale. Des résultats numériques pour le nombre de Nusselt, le nombre de Sherwood, les courbes de stabilité neutre sont présentés dans le cas des nombres de Lewis entre 1 et 10 et des rapports de flottement entre $-0,5$ et 4. Pour un transfert de masse aidant l'écoulement, les résultats indiquent que les nombres de Nusselt et de Sherwood sont plus grands que ceux de la convection thermique pure et que l'écoulement est plus sensible à l'instabilité de vortex, tandis que pour le transfert de masse s'opposant à l'écoulement on constate un comportement inversé. Le nombre de Rayleigh thermique critique augmente lorsque le nombre de Lewis diminue.

STRÖMUNG UND WIRBELINSTABILITÄT BEI HORIZONTALER NATÜRLICHER KONVEKTION IN EINEM PORÖSEN MEDIUM

Zusammenfassung—Die Strömung und die Wirbelinstabilität bei natürlicher Konvektion in einem porösen Medium, welche von gleichzeitiger Wärme- und Stoffübertragung in einer zu einer horizontalen, Oberfläche benachbarten Grenzschicht herrührt, wird untersucht. Numerische Ergebnise für die Nusselt-Zahl, die Sherwood-Zahl und die neutralen Stabilitätskurven werden für einen Lewish-Zahl-Bereich von 1 bis 10 und ein Auftriebsverhältnis im Bereich von $-0,5$ bis 4 vorgestellt. Wird die Strömung durch Stoffübertragung unterstützt, so sind, wie die Ergebnisse zeigen, die Nusselt-Zahl und die Sherwood-Zahl höher als bei reiner thermischer Konvektion, und die Strömung ist mehr empfänglich für die Wirbvelinstabilität. Behindert die Stroffbertragung die Strömung, tritt das entegegengesetzte Verhalten auf. Es ergibt sich, daß die kritische thermische Rayleigh-Zahl mit fallender Lewish-Zahl zunimmt.

ТЕЧЕНИЕ И ВИХРЕВАЯ НЕУСТОЙЧИВОСТЬ ГОРИЗОНТАЛЬНОЙ ЕСТЕСТВЕННОЙ КОНВЕКЦИИ В ПОРИСТОЙ СРЕДЕ ПРИ СОВМЕСТНОМ ДЕЙСТВИИ ТЕПЛОВОЙ И КОНЦЕНТРАЦИОННОЙ КОНВЕКЦИИ

Аннотация—Анализируется течение и вихревая неустойчивость естественной конвекции в пористой среде, вызванные одновременной диффузией тепла и массы в пограничный слой, примыкающий к горизонтальной поверхности. Представлены численные результаты для чисел Нуссельта, Шервуда, а также кривые нейтральной устойчивости, полученные в диапазоне чисел Льюиса от 1 до 10 и при отношении подъемных сил от $-0,5$ до 4. Показано, что при массопереносе, сонаправленном с течением, числа Нуссельта и Шервуда выше по сравнению со случаем чистой тепловой конвенции, течение менее устойчиво по отношению к вихревым возмущениям, в то время как для массопереноса, препятствующего течению, справедлива обратная тенденция. Найдено, что критическое тепловое число Рэлея возрастает с уменьшением числа Льюиса.